

# Mesoscopic Effects in the Thermopower of Dilute AuFe Alloys

C. Strunk,<sup>\*</sup> G. Neuttiens,<sup>†</sup> M. Henny,<sup>\*</sup> C. Van Haesendonck,<sup>†</sup> and C. Schönenberger<sup>\*</sup>

<sup>\*</sup>Institut für Physik, Universität Basel Klingelbergstr. 82, CH-4056 Basel, Switzerland

<sup>†</sup>Laboratorium voor Vaste-Stoffysica en Magnetisme, Katholieke Universiteit Leuven, Celestijnenlaan 200 D, B-3001 Leuven, Belgium

**Summary:** We have employed electron heating experiments and noise thermometry to perform quantitative measurements of the thermopower in mesoscopic samples. This new measuring technique allows to detect finite size effects in the thermopower of narrow AuFe wires with an Fe concentration ranging from 50 to 3000 ppm. The size effects emerge when reducing the width of the wires below  $\simeq 300$  nm. Our observations can be understood in terms of a magnetic anisotropy which affects the spins close to the surface of the sample. The spin glass freezing at lower temperatures suppresses the size effects.

## 1 Introduction

When transition metal impurities are introduced into noble metals the scattering of the conduction electrons at the impurity spins leads to important changes of their low temperature properties [1]. For small concentrations below  $\simeq 100$  ppm of the magnetic dopant the Kondo effect gives rise to a logarithmic increase of the resistivity  $\rho(T)$ . Below the Kondo temperature  $T_K$  a compensation cloud of conduction electrons is formed around the impurity spins which gradually screens their magnetic moment. At higher concentrations ( $\sim 1\text{at.}\%$ ) the Ruderman-Kittel-Kasuya-Yosida (RKKY) interaction between the randomly distributed impurity spins competes with the Kondo effect and causes a freezing of the impurity spins into a disordered configuration called a spin glass. This is reflected by the appearance of a typical broad maximum in  $\rho(T)$  since the spin scattering rate again decreases at the lowest temperatures due to the freezing process.

Recent experimental work has addressed the existence of intrinsic length scales for both the Kondo effect and the spin glass freezing process [2, 3, 4, 5, 6]. The results have so far been controversial: While some groups [2, 3] report a

pronounced depression of the Kondo slope with decreasing film thickness and wire width, other authors claim that the observed size effects are small and can moreover be explained quantitatively in terms of disorder enhanced electron-electron interaction effects [5, 6]. It was also noted that structural disorder may have an important influence on the spin dependent part of  $\rho(T)$  for Kondo alloys [7] as well as for more concentrated spin glass alloys where a damping of the RKKY interaction occurs [6, 8].

It was initially suggested [2] that the Kondo effect should be affected if at least one linear dimension of the sample becomes smaller than the size  $\xi_K = \hbar v_F / k_B T_K$  of the Kondo screening cloud which is about  $10 \mu\text{m}$  for AuFe. Very recent calculations, however, indicate [9] that it is the ratio of  $k_B T_K$  to the level spacing  $\delta$  which governs the suppression of the Kondo effect. Because the level spacing is determined by the Fermi wavelength and sample volume  $V$ , it is not the smallest linear dimension that sets the scale but  $V < \pi \xi_K / k_F^2$ . This type of size effects is apparently restricted to ultrasmall grains with volumes  $V < (15 \text{ nm})^3$  for AuFe.

In a different theoretical approach it has been shown that in the single impurity limit spin-orbit interactions can induce a size dependent magnetic anisotropy which results in a size dependent resistivity [10]. For the impurity spins close to the sample surface the spin orbit scattering removes the degeneracy of the spin states of the impurity and at low temperature the spin is frozen in the ground state. Depending on the value of the impurity spin, the ground state is either a singlet (e.g. Fe or Cr with  $S = 2$ ) or a doublet (e.g. Mn with  $S = 5/2$ ) showing no or reduced dynamics at low temperatures. For more disordered samples, an interplay between weak localization and the Kondo effect has been predicted which can account for both a disorder effect and a size effect [11].

In order to address the open questions related to the size effects, it is obviously interesting to look at other transport properties which are affected by the spin scattering. An excellent candidate is the thermoelectric power (TEP),  $S(T)$ , which is known to be strongly enhanced in dilute magnetic alloys. While in bulk Au  $S(T)$  is positive and small [12], it switches sign upon adding Fe impurities and its absolute value can be as high as  $15 \mu\text{V/K}$ . Further increase of the Fe concentration into the spin glass regime again reduces  $|S(T)|$  [13].

We have developed a new method for thermopower measurements on mesoscopic samples. The recently observed asymmetry of the differential resistance as a function of the heating current [14, 15] together with noise thermometry for the measurement of the electron temperature allows a direct and quantitative determination of the size dependent part of thermopower in dilute AuFe wires [16]. A clear reduction of  $|S(T)|$  is observed, when the width of the AuFe wires is reduced from 300 down to 100 nm. Our measurements allow to directly test the theoretical models which link the size dependence to a surface induced magnetic anisotropy [10].

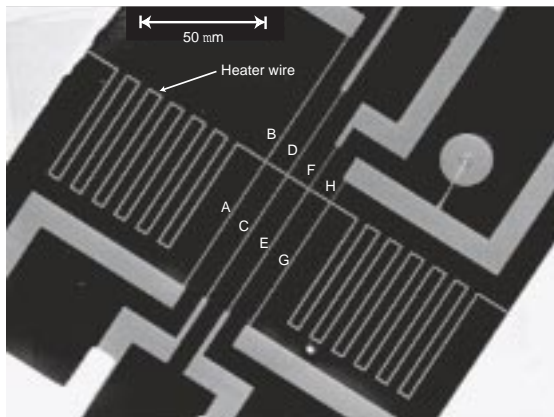


**Figure 1** Scanning electron micrograph of a typical sample. The four different thermocouples are labeled  $AB$ ,  $CD$ ,  $EF$ , and  $GH$ .

## 2 Sample Design

The samples consist of pairs of AuFe wires of different width (forming thermocouples) connected at one end to a meandering wire which serves as a heater with resistance  $R_H$  (see Fig. 1). The electron temperature  $T_H$  in the heater is raised above the substrate temperature  $T_S$  when a  $dc$  current  $I$  flows through the heater. The other ends of the thermocouple wires are connected to large contact pads which are assumed to remain at  $T_S$ .

The wires  $A, C, E, G$  on one side of the 510 nm wide heater have the same nominal width of  $300 \pm 15$  nm and serve as a reference to detect small changes of the thermopower when varying the width of the wires labeled  $B, D, F, H$  on the other side. The latter wires have a width  $w$  of 305, 220, 140, and 105 nm, respectively, and their length increases with increasing  $w$  to keep the thermal conductance of all wires constant. The length of the narrowest wires as well as the distance between the junctions is 10  $\mu\text{m}$  while the total length of the meandering heater is 1.4 mm. This geometry provides a nearly flat profile of  $T_H$  along the heater except at both ends of the heater close to the large contact pads [17]. We note that – regardless of the temperature profile in the sample – in the absence of a size effect in  $S(T)$  no thermovoltages are expected to develop across our mesoscopic thermocouples made entirely from AuFe. The samples have been prepared by electron beam lithography and evaporation of 99.999% pure Au. In a second step Fe ions have been implanted at several energies to provide a reason-

ably constant doping profile perpendicular to the film [5]. Two series of samples were prepared having nominal Fe concentrations of 50 and 3000 ppm, respectively. Prior to implantation, the 30 nm thick films had a sheet resistance  $R_{\square}$  of 0.3  $\Omega$  at 4.2 K. After implantation  $R_{\square}$  of the 50 ppm Kondo samples remained unchanged while  $R_{\square}$  of the 3000 ppm spin glass samples increased to 0.7  $\Omega$ . This corresponds to an elastic mean free path  $l_{el}$  of 90 and 40 nm, respectively. SEM and AFM images indicate that the films are polycrystalline with a grain size (20-30 nm) considerably smaller than the wire width. We emphasize that the size dependence, which we will report in this paper, cannot be explained by a simple disorder effect since all wires are prepared simultaneously, resulting in a value of  $l_{el}$  which is independent of the wire width. Most of the measurements have been performed in a  $^3\text{He}$  cryostat at a bath temperature of 300 mK.

### 3 Measuring Method

The idea of our thermopower experiment is the following: If a current  $I$  is sent through the heater wire the electron temperature in the heater rises above the substrate temperature  $T_S$ . The temperature at the thermocouple junctions  $T_J$  will be slightly lower than the average temperature of the heater  $T_H$  because of the finite thermal conductance of the thermocouple wires. The resulting thermoelectric voltage across the thermocouples will be symmetric in  $I$  since  $T_J(I)$  is symmetric in  $I$ :

$$V_{th}(I) = \int_{T_S(I)}^{T_J(I)} \Delta S(T) dT \quad , \quad (3.1)$$

where  $\Delta S(T) = S_{wide}(T) - S_{narrow}(T)$  is the thermopower difference between the wide and narrow wire of the thermocouple. In order to increase the sensitivity of our measurements, we measure the differential resistance  $dV/dI$  rather than  $V(I)$  across our thermocouples. Since  $V_{th}(I)$  is symmetric in  $I$ ,  $dV/dI$  will predominantly be antisymmetric in  $I$ . According to Eq. (3.1), the antisymmetric part of  $dV/dI$  is directly linked to  $\Delta S(T)$ :

$$\frac{dV_{th}}{dI} = \Delta S(T_J) \frac{dT_J}{dI} - \Delta S(T_S) \frac{dT_S}{dI} \quad . \quad (3.2)$$

The second term in Eq. (3.2) represents the contribution of the also elevated substrate temperature  $T_S$  at higher currents. To extract  $\Delta S(T)$ , Eq. (3.2) has to be solved selfconsistently. Similar cross-shaped geometries have been used to measure mesoscopic TEP fluctuations in GaAs quantum wires [18] and the TEP of quantum point contacts [19]. However, in these experiments the electron temperature has not been measured independently.

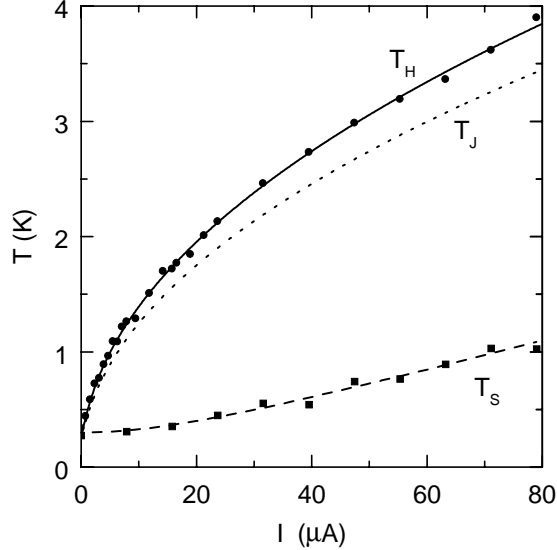


**Figure 2** Electron temperatures  $T_H(I)$  of the heater and  $T_S(I)$  of the substrate monitor wire together with fits as described in the text. The dotted line corresponds to a value of  $a = 0.0247 \text{ K}^b/\mu\text{A}^2$  and indicates the temperature  $T_J(I)$  at the thermocouple junction  $GH$ .

#### 4 Electron Heating and Noise Thermometry

The average temperature in the heater wire  $T_H(I)$  has been determined by measuring the spectral density  $S_V(I) = 4k_B T_H(I) R_H$  of the voltage fluctuations across the heater wire as a function of current bias [17]. For typical heater resistances  $R_H$  of 1-2 k $\Omega$  the electron temperature could be determined with an accuracy of about 50 mK. Figure 2 shows an example of  $T_H(I)$  for the 3000 ppm sample together with a fit corresponding to the semi-empirical form  $T_H(I) = (aI^2 + T_0^b)^{1/b}$ , where  $T_0 = 0.3 \text{ K}$  is the temperature of the sample stage. The parameters for the best fit were  $a = 0.0386 \text{ K}^b/\mu\text{A}^2$  and  $b = 4.1$ . In agreement with previous electron heating experiments in this temperature range [20], we find that  $b$  ranges from 4.0 to 4.3 for different samples. A detailed discussion of the physical origin of the exponent  $b$  is beyond the scope of this paper and will be given elsewhere. With a heating current of 80  $\mu\text{A}$  electron temperatures up to 4 K have been achieved.

The temperature at the junction  $T_J(I)$  has been determined by a numeri-

cal solution of the heat diffusion equation in the presence of electron-phonon scattering based on Ref. [21]:

$$\frac{\pi^2}{6} \frac{d^2 T_{el}^2}{d^2 x} = - \left( \frac{e|\vec{E}|}{k_B} \right)^2 + (T_{el}^b(x) - T_S^b) \quad (4.3)$$

Here,  $\vec{E}$  denotes the electric field in the heater wire and  $\gamma = (eR_H/k_B L_H)^2/a$  characterizes the strength of the electron-phonon interaction, where  $L_H$  is the length of the heater. The calculation uses the measured  $T_H(I)$  curve to take into account the cooling through the electron-phonon scattering and the result is indicated by the dotted line in Fig. 2. A comparison of the current dependence of the resistivity for the different sections of the heater wire confirms that the local reduction of  $T_H$  remains smaller than 10 %. For the highest currents a power of  $\simeq 10 \mu\text{W}$  is dissipated in the heater, which is sufficient to also raise the substrate temperature up to  $T_S \simeq 1 \text{ K}$ . The open symbols in Fig. 2 show  $T_S$  measured on an independent Au wire patterned close to the AuFe sample while current is sent through the heater wire. The dashed line is a fit of the form  $T_S = \sqrt{a'I^2 + T_0^2}$  with  $a' = 0.00017 \text{ K}^2/\mu\text{A}^2$ . This functional dependence is expected since the thermal coupling between the sample stage of the cryostat and the substrate is metallic with a thermal conductance depending linearly on temperature.

## 5 Thermopower Measurements

In order to detect the response of the thermocouples a small ac current of  $1 \mu\text{A}$  and 116 Hz is added to the dc heating current  $I$  and the corresponding ac voltage is detected with a lock-in amplifier. We first measured in detail the  $dV/dI$  signal for the 50 ppm thermocouples. As shown in the inset of Fig. 3, the thermocouple  $EF$  clearly reveals the presence of a signal which is antisymmetric in  $I$  and is of the order of  $1 \text{ m}\Omega$ . The antisymmetric signal increases when the difference in width  $\Delta w$  increases, which can be linked to a decrease of the thermopower in the narrower AuFe wires. According to the Gorter-Nordheim rule [12] the measured TEP in our Kondo samples is strongly reduced by the non-magnetic scattering. The reduction factor is given by the ratio of the total resistivity  $\rho_{tot}$  and the resistivity contribution  $\rho_{Fe}$  [22] of the Fe impurities. Relying on the reported resistivity  $\rho_{Fe}$  for bulk samples [1, 23], we estimate  $\rho_{tot}/\rho_{Fe} \simeq 12$ . According to Eq. (3.2) and the available data for the thermopower in bulk Kondo alloys [13] we find that for the thermocouple  $EF$  the observed thermopower signal  $\Delta S(T)$  is of the order of 6% of the bulk thermopower. Unfortunately, the poor signal to noise ratio for our Kondo samples does not allow to draw more quantitative conclusions concerning the width dependence of the thermopower.

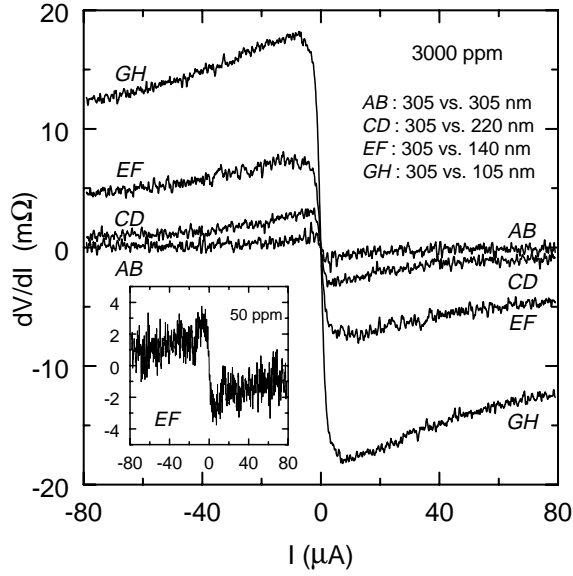


**Figure 3** Antisymmetric part of the differential resistance for the different thermocouples. Voltage contact  $V_+$  was connected to one of the reference wires  $A$ ,  $C$ ,  $E$ ,  $G$  (nominal  $w = 300$  nm) while  $V_-$  was connected to one of the narrow wires  $B$ ,  $D$ ,  $F$ ,  $H$  ( $w = 305$ ,  $220$ ,  $140$ , and  $105$  nm, respectively). Trace  $AB$  is an average of several  $300/300$  nm combinations. Inset: Asymmetric part of  $dV/dI$  for thermocouple  $EF$  of a sample with  $50$  ppm Fe.

For the  $3000$  ppm samples a comparison with the data for bulk alloys [1, 23] indicates that  $\rho_{tot} \simeq \rho_{Fe}$  for our relatively clean samples. Consequently, the thermoelectric voltages are considerably larger than for the Kondo samples and a quantitative data analysis becomes possible. Figure 3 shows the antisymmetric part of the  $dV/dI$  signal from the thermocouples  $AB$ ,  $CD$ ,  $EF$ , and  $GH$ , respectively (see Fig. 1). For the thermocouple  $GH$  which has the largest difference in width  $\Delta w$ ,  $dV/dI$  rises very sharply from zero, shows a maximum around  $7 \mu\text{A}$  and slowly decreases for higher currents. For decreasing  $\Delta w$  in the thermocouples  $EF$  and  $CD$  the asymmetry is systematically reduced while the overall shape of the  $dV/dI$  signal remains similar. For the thermocouple  $AB$ , where  $\Delta w$  is nominally zero, a residual small asymmetry is observed which is of random sign for different samples and can be attributed to small size differences related to imperfections of the lithographic patterning.

In Fig. 4 we have plotted the temperature dependence of  $\Delta S(T)$  for the different  $3000$  ppm thermocouples according to Eq. (3.2). For the Kondo as well as

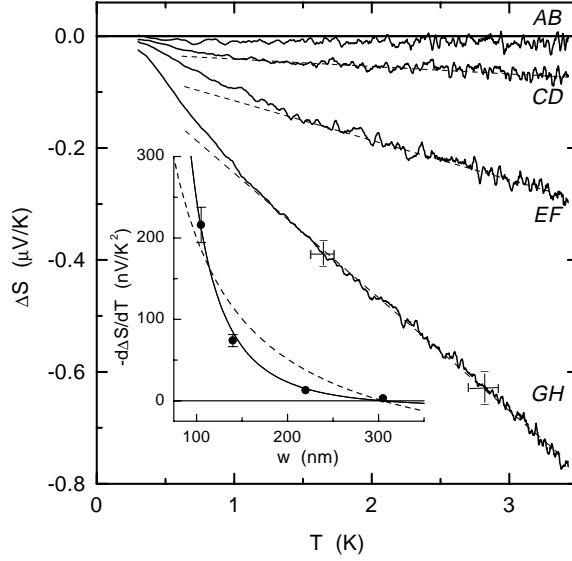


**Figure 4** Difference in thermopower as function of temperature for varying difference in wire width. The dashed lines illustrate the linear behavior of  $\Delta S(T)$  above 1.5 K. The error bars indicate the uncertainty introduced by the correction of the temperature profile. Inset: Slope of  $|\Delta S(T)|$  at  $T = 3$  K as a function of the width of the narrow wire. The lines are best fits of a  $1/w^3$  (solid) and a  $1/w$  (dashed) dependence.

for the spin glass samples  $\Delta S(T) = S_{wide} - S_{narrow}$  is negative, implying that  $|S(T)|$  becomes smaller when reducing the width of the wires. For the 3000 ppm data (see Fig. 4)  $\Delta S(T)$  displays a nearly linear variation above 1.5 K which is close to the spin glass freezing temperature  $T_f$  for 3000 ppm [1]. The inset of Fig. 4 shows  $|d\Delta S(T)/dT|$  for the linear regime as a function of the width of the narrower wire of the thermocouples. At lower temperatures  $|\Delta S(T)|$  decreases more rapidly and is nearly zero at 0.4 K. The measured values of  $|\Delta S(T)|$  range up to  $0.8 \mu\text{V/K}$  which should be compared with the value  $|S(T)| \simeq 7 \mu\text{V/K}$  observed for bulk AuFe samples with a comparable Fe concentration [13]. On the other hand, the thermoelectric voltages become very small when both wires forming the thermocouples are wider than 300 nm. We therefore conclude that for Kondo as well as for spin glass AuFe wires the thermopower is significantly reduced when reducing the width down to 100 nm.

## 6 Discussion

What is the origin of the size dependence? We have checked that the asymmetric  $dV/dI$  is absent in undoped samples. For the more dilute alloys ( $\leq 500$  ppm) a magnetic field of 17 T completely suppresses the asymmetry. This proves that the observed thermoelectric voltages are indeed related to the magnetic scattering. Since the size effects are also present in the Kondo samples, it is reasonable to link them to a single impurity effect. The direct finite size effect discussed in Ref. [9] can most probably be excluded since the level spacing in our samples is much smaller than  $\hbar V_F/k_B T_K$ . Since our samples are relatively clean and phase coherent effects like weak localization are strongly suppressed in the highly Fe doped samples it is also unlikely that the interplay between the Kondo effect and weak localization as discussed in [11] is responsible for the observed size effects.

What remains is the spin-orbit induced magnetic anisotropy as proposed in Ref. [10]. For relatively high temperatures  $T \geq T_f$ , a considerable fraction of the magnetic impurity spins is still free to flip independently in the more concentrated spin glass wires and are therefore expected to be sensitive to the spin-orbit induced suppression of the spin dynamics in the vicinity of the sample surface. The observed size effect in the thermopower is relatively small ( $\simeq 10\%$ ) which is consistent with the apparent absence of a size dependence in the less sensitive resistivity measurement by Chandrasekhar *et al.* [5]. Although we find a size dependence when reducing the wire width, it is much smaller than the drastic effect in two-dimensional films reported in the early experiments of Refs. [2, 3]. In addition, we have found [15] that the thermopower of a 1  $\mu\text{m}$  wide Au/AuFe thermocouple with 4000 ppm Fe is very close to its bulk value [13]. The survival of the Kondo effect in two-dimensional films indicates that two orthogonal sample surfaces as are present in narrow wires are needed to efficiently quench the spin dynamics by the surface induced magnetic anisotropy.

As shown in the inset of Fig. 4,  $|d\Delta S(T)/dT|$  increases more rapidly with decreasing width ( $\propto 1/w^3$ ) for the 3000 ppm thermocouples than the predicted  $1/w$  dependence of the slope of the Kondo resistivity [10]. At temperatures below  $T_f$  the spin flip scattering by the individual magnetic moments is suppressed by the strong internal fields which are present in the spin glass phase. This is consistent with the vanishing of the  $\Delta S(T)$  below 0.4 K (see Fig. 4).

## Acknowledgements

We are much indebted to Y. Bruynseraede, V. Chandrasekhar, J. Eom, J. Devreese, V. Fomin, V. Gladilin, and A. Zawadowski for stimulating discussions and to H. Pattyn, L. Lanz and H. Birk for their help with the sample preparation and the measurement setup. The work at Basel has been supported by the Swiss National Science Foundation. The work at Leuven has been supported

by the Fund for Scientific Research - Flanders (FWO) as well as by the Flemish Concerted Action (GOA) and the Belgian Inter-University Attraction Poles (IUAP).

## Bibliography

- [1] For a recent review see, e.g.: J. A. Mydosh, *Spin glasses, An experimental introduction* (Taylor & Francis, London, 1993).
- [2] G. Chen and N. Giordano, Phys. Rev. Lett. **66**, 209 (1991).
- [3] J. F. DiTusa *et al.*, Phys. Rev. Lett. **68**, 678 (1992).
- [4] K. R. Lane, M. Park, M. S. Isaacson, and J. M. Parpia, Phys. Rev. **B51**, 945 (1995).
- [5] V. Chandrasekhar *et al.*, Phys. Rev. Lett. **72**, 2053 (1994).
- [6] G. Neuttiens *et al.*, Europhys. Lett. **34**, 617 (1996).
- [7] M. A. Blachly and N. Giordano, Europhys. Lett. **27**, 687 (1994).
- [8] R. Buchmann, H. P. Falke, H. P. Jablonski, and E. F. Wassermann, Phys. Rev. B **17**, 4315 (1978).
- [9] W. B. Thimm, J. Kroha, and J. van Delft, Phys. Rev. Lett. **82**, 2143 (1999).
- [10] O. Újsághy, A. Zawadowski, and B. L. Gyorffy, Phys. Rev. Lett. **76**, 2378 (1996); O. Újsághy and A. Zawadowski, Phys. Rev. B **57**, 11 598 (1998) and Phys. Rev. B **57**, 11 609 (1998) ; V. Fomin *et al.*, Sol. Stat. Comm. **106**, 293 (1998).
- [11] I. Martin, Y. Wan, and P. Phillips, Phys. Rev. Lett. **78**, 114 (1997).
- [12] R. D. Barnard, *Thermoelectricity in metals and alloys* (Taylor & Francis, London, 1972).
- [13] D. K. C. MacDonald, W. B. Pearson, and I. M. Templeton, Proc. Roy. Soc. **A266**, 161 (1962).
- [14] J. Eom *et al.*, Phys. Rev. Lett. **77**, 2276 (1996).
- [15] G. Neuttiens *et al.*, Europhys. Lett. **42**, 185 (1998).
- [16] C. Strunk *et al.*, Phys. Rev. Lett. **81**, 2982 (1998).
- [17] M. Henny *et al.*, Appl. Phys. Lett. **71**, 773 (1997).
- [18] B. L. Gallagher *et al.*, Phys. Rev. Lett. **64**, 2058 (1990).
- [19] L. W. Molenkamp *et al.*, Phys. Rev. Lett. **65**, 1052 (1990).
- [20] See, e.g.: G. Bergmann, Wei Wei, Yao Zhou, and R. M. Mueller, Phys. Rev. B **41**, 7386 (1990), J. F. DiTusa *et al.*, Phys. Rev. Lett. **68**, 1156 (1992).
- [21] K. E. Nagaev, Phys. Rev. B **52**, 4740 (1995).
- [22] Here we assume that the magnetic TEP dominates all other contributions, which is well justified for dilute magnetic alloys [12].
- [23] O. Laborde and P. Radhakrishna, Sol. Stat. Comm. **9**, 701 (1971).